ISBN: 978-3-95450-219-6 ISSN: 2226-0366 doi: 10.18429/JACoW-LINAC2024-MOPB026

DESIGN OF A QUADRIPARTITE WAKEFIELD STRUCTURE FOR FREE ELECTRON LASER APPLICATIONS

Y. Ji[1], C. Lei[1], J. Shao[1,*], Y. Yu[1], J. Sun[2], Zongbin Li[1], L. He[1], H. Wang[1], J. Wei[1], W. Wei[1], W. Wang[1], J. Yang[2], W. Zhang[2], X. Yang[2]
[1]Institute of Advanced Science Facilities, Shenzhen, China
[2]Dalian Institute of Chemical Physics, Dalian, China

Abstract

Wakefield structures are broadly employed in free electron laser (FEL) facilities for beam manipulation. Compared with cylindrical geometries, planar structures are typically preferred due to their increased flexibility, allowing for tunable wakefield strength through gap adjustment. However, these planar configurations can induce time-dependent quadrupole wakefields, which require careful compensation in various applications. To address this issue, we propose a novel structure design incorporating four identical corrugated elements which are independently controllable. By adjusting the gaps between orthogonal pairs, the quadrupole wakefield can be either fully compensated to avoid emittance growth or significantly amplified to enhance beam mismatch for slice lasing control. This manuscript presents both the physical and mechanical design of the proposed structure, as well as the planned proof-of-principle experiment.

INTRODUCTION

Wakefields are induced when a charged bunch traverses a corrugated or dielectric pipe. Structure-based wakefield acceleration represents a promising approach to achieve gradients significantly higher than those attained by conventional techniques [1–3]. Furthermore, wakefield have been demonstrated to be effective tools for beam manipulation in FELs, where the short-range wakefield from the bunch head can alter the longitudinal or transverse momentum of the tail [4–18]. Initially, wakefield structures were employed in FELs as dechirpers to mitigate the linear energy chirp introduced for magnetic bunch compression [4, 5, 7]. Since then, these structures have been adapted for a broader range of applications, such as passive linearization [6, 13], slice lasing control [8, 10–12, 14, 15], and passive deflection [9, 17, 18].

The Shenzhen Superconducting Soft X-Ray Free-Electron Laser (S^3FEL) is a newly proposed, high repetition-rate FEL facility featuring multiple undulator lines that lase in the 1–30 nm range [19]. Wakefield structures are under development to serve as dechirpers and as key components for advanced FEL modes. Their performance is crucial to achieving high lasing quality in S^3FEL.

Most FEL facilities apply planar structures with two corrugated plates, where the longitudinal wakefield strength can be adjusted by varying the gap. However, quadrupole wakefield is introduced in addition to the longitudinal wakefield due to the asymmetric geometry. The time-dependent quadrupole wakefield can cause beam mismatch and emittance growth, which usually require compensation by placing two pairs of plates orthogonally and maintaining nearly symmetric average β functions throughout the structures [7]. Conversely, purposely enhancing beam mismatch via the quadrupole wakefield can be exploited for slice lasing control, by individually matching the slices into different undulators [10, 11]. Consequently, it would be desirable to introduce a structure that provides flexible and independent control of both longitudinal and quadrupole wakefield.

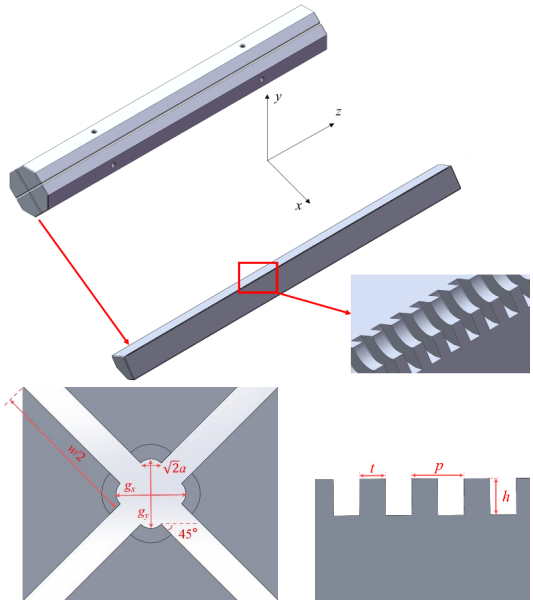

Figure 1: Schematic layout of the quadripartite wakefield structure.

Therefore, we propose a novel wakefield structure consisting of four identical elements. By adjusting the gaps between orthogonal pairs, the quadrupole wakefield can be either fully compensated or significantly amplified, while the impact to the longitudinal wakefield is moderate. Such design allows for flexible manipulation of bunch slice properties for various applications.

PHYSICAL DESIGN

The quadripartite wakefield structure comprises four identical corrugated plates, each independently controlled by a pair of high-precision motors, as illustrated in Fig. 1. The corrugation of each plate can be designed either as a quarter-circle curve or flat, without affecting the fundamental work-

* shaojiahang@mail.iasf.ac.cn

ISBN: 978-3-95450-219-6 ISSN: 2226-0366 doi: 10.18429/JACoW-LINAC2024-MOPB026

Table 1: Parameters of the Quadripartite Wakefield Structure

Parameter	Value	Unit
Corrugation period p	0.5	mm
Corrugation length t	0.25	mm
Corrugation depth h	0.5	mm
Effective horizontal gap g_x	1.4	mm
Effective vertical gap g_y	1.4	mm
Slot length w	7	mm
Pipe radius a when fully closed	0.5	mm

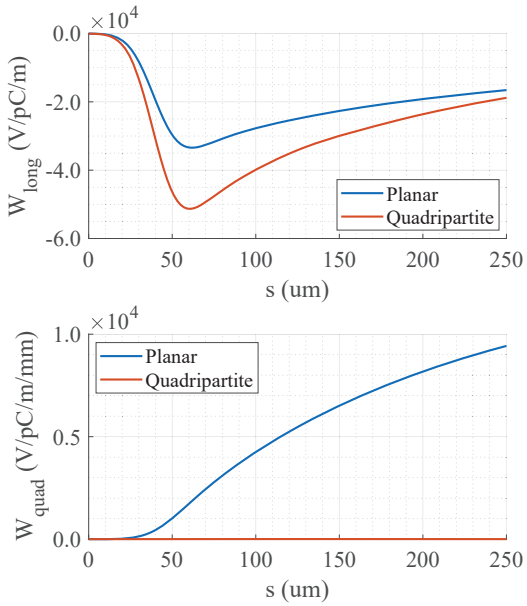

Figure 2: Comparison of the longitudinal wakefield (top) and the quadrupole wakefield (bottom) between the planar and the quadripartite structures when $g_x = g_y = 1.4$ mm.

ing principle. In the following physical analysis, the curved configuration is employed with its key parameters listed in Table 1.

ECHO3D [20] and CST wakefield solver [21] have been used to simulate the wakefield of the proposed structure, and their results have been benchmarkded against each other. Figure 2 and 3 illustrate the simulation results for an on-axis charged beam with a Gaussian temporal distribution and an rms bunch length of 12 µm. When $g_x = g_y$, the quadrupole wakefield is not induced due to the structure symmetry. Furthermore, compared to the planar structure using the same corrugation parameters p, t, and h, the quadripartite structure produces ~50% stronger longitudinal wakefield, leading to a shorter required length to mitigate a given energy chirp. Conversely, when g_x is fixed as 1.4 mm and g_y is adjusted, the quadrupole wakefield can be significantly enhanced to either direction, while the variation in the longitudinal wakefield remains moderate.

MECHANICAL DESIGN

To fully leverage these advantages, the four corrugated plates must be positioned with high precision, making the

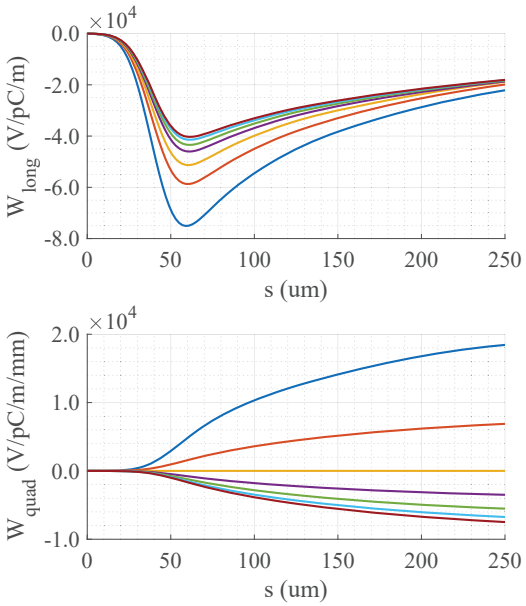

Figure 3: Simulation results of the quadripartite structures when $g_x = 1.4$ mm and $g_y = 1.0$–2.2 mm, as the longitudinal wakefield (top) from strong to weak and the quadrupole wakefield (bottom) from positive to negative.

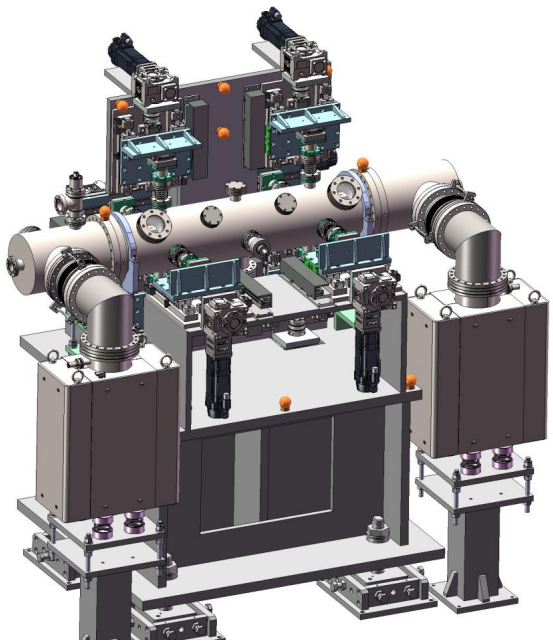

Figure 4: Layout of the prototype.

mechanical design critical for the proposed structure. Consequently, a prototype structure (Fig. 4) featuring 1 m-long aluminium corrugation plates has been designed for beam test at Dalian Coherent Light Source (DCLS, Fig. 5) [22] to benchmark the simulation results and validate engineering aspects.

For manufacturing simplicity, the corrugation has been designed as flat configuration, and each 1 m-long plate are divided into four 0.25 m sections, which are bolted onto a main girder, as illustrated in Fig. 6. To match the realistic

ISBN: 978-3-95450-219-6 ISSN: 2226-0366 doi: 10.18429/JACoW-LINAC2024-MOPB026

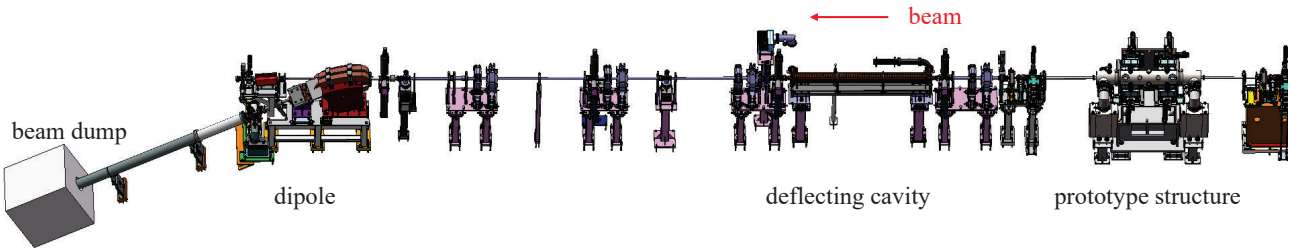

Figure 5: Schematic layout of the proof-of-principle experiment.

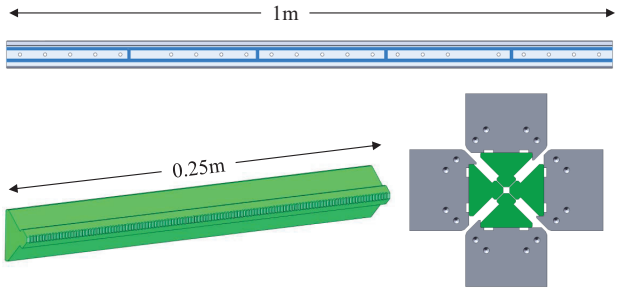

Figure 6: Top: bottom view of the main girder; bottom left: the corrugation plate; bottom right: cross-section of the corrugation assembly.

beam condition, p, t, and h are respectively designed to be 2 mm, 1 mm, and 1 mm, and the minimal effective gap is set to be 3.5 mm. Alignment of the sections on the same girder will be achieved through precise trimming. Venting slots are incorporated into both the corrugation sections and the main girders to maintain ultra-high vacuum. With two 400 L/s ion pumps places at the ends, the vacuum inside the chamber is simulated to be better than 1×10^{-7} Pa.

Each 1 m-long plate is controlled by two synchronized high-precision motors. The misalignment between the main girders due to assembly, deforming, and motor position error is required to be less than 50 μm.

PLANNED PROOF-OF-PRINCIPLE EXPERIMENT

The proof-of-principle experiment is scheduled to be conducted in DCLS where low-emittance electron beam is produced by an S-band 1.6-cell photocathode RF gun and accelerated to 300 MeV via six S-band 3 m-long linacs.

The prototype wakefield structure will be installed between the undulator beamline and the downstream diagnostics section. Diagnostics involved in the experiment will include a 12 MV S-band deflecting cavity, a dipole magnet with beam dump, and several beam profile monitors. In alignment with methodologies established in previous studies [5, 23], the longitudinal, dipole, and quadrupole wakefields will be inferred from the longitudinal phase space, beam tail offset, and slice transverse size, respectively. Beam dynamics simulation has been thoroughly conducted to obtain the proper lattice settings for the experiment.

CONCLUSION

A quadripartite wakefield structure comprising four identical corrugated elements has been proposed for FEL applications. The independently controllable plates enable a flexible configuration to control the longitudinal and quadrupole wakefields. A prototype structure has been designed and is currently under fabrication. The proof-of-principle experiment is scheduled to take place at DCLS in 2025.

ACKNOWLEDGEMENTS

The authors would like to thank the support from Dalian Coherent Light Source. This work is also supported by the Talent Program of Guangdong Province (No.2021QN02G685).

REFERENCES

[1] B. O'Shea *et al.*, "Observation of acceleration and deceleration in gigaelectron-volt-per-metre gradient dielectric wakefield accelerators", *Nat. Commun.*, vol. 7, p. 12763, 2016. doi:10.1038/ncomms12763

[2] C. Jing *et al.*, "Electron acceleration through two successive electron beam driven wakefield acceleration stages", *Nucl. Instrum. Methods Phys. Res. A*, vol. 898, pp. 72–76, 2018. doi:10.1016/j.nima.2018.05.007

[3] D. Merenich *et al.*, "Breakdown insensitive acceleration regime in a metamaterial accelerating structure", *Phys. Rev. Accel. Beams*, vol. 27, p. 041301, 2024. doi:10.1103/PhysRevAccelBeams.27.041301

[4] K. Bane and G. Stupakov, "Corrugated pipe as a beam dechirper", *Nucl. Instrum. Methods Phys. Res. A*, vol. 690, pp. 106–110, 2012. doi:10.1016/j.nima.2012.07.001

[5] P. Emma *et al.*, "Experimental demonstration of energy-chirp control in relativistic electron bunches using a corrugated pipe", *Phys. Rev. Lett.*, vol. 112, p. 034801, 2014. doi:10.1103/PhysRevLett.112.034801

[6] H. Deng *et al.*, "Experimental demonstration of longitudinal beam phase-space linearizer in a free-electron laser facility by corrugated structures", *Phys. Rev. Lett.*, vol. 113, p. 254802, 2014. doi:10.1103/PhysRevLett.113.254802

[7] Z. Zhang *et al.*, "Electron beam energy chirp control with a rectangular corrugated structure at the Linac Coherent Light Source", *Phys. Rev. ST Accel. Beams*, vol. 18, p. 010702, 2015. doi:10.1103/PhysRevSTAB.18.010702

[8] A. Lutman *et al.*, "Fresh-slice multicolour X-ray free-electron lasers", *Nat. Photonics*, vol. 10, p. 745–750, 2016. doi:10.1038/nphoton.2016.201

ISBN: 978-3-95450-219-6 ISSN: 2226-0366 doi: 10.18429/JACoW-LINAC2024-MOPB026

[9] S. Bettoni *et al.*, "Temporal profile measurements of relativistic electron bunch based on wakefield generation", *Phys. Rev. Accel. Beams*, vol. 19, p. 021304, 2016. doi:10.1103/PhysRevAccelBeams.19.021304

[10] W. Qin *et al.*, "Matching-based fresh-slice method for generating two-color x-ray free-electron lasers", *Phys. Rev. Accel. Beams*, vol. 20, p. 090701, 2017. doi:10.1103/PhysRevAccelBeams.20.090701

[11] Y. Chao *et al.*, "Control of the lasing slice by transverse mismatch in an X-ray free-electron laser", *Phys. Rev. Lett.*, vol. 121, p. 064802, 2018. doi:10.1103/PhysRevLett.121.064802

[12] A. Lutman *et al.*, "High-power femtosecond soft x rays from fresh-slice multistage free-electron lasers", *Phys. Rev. Lett.*, vol. 120, p. 264801, 2018. doi:10.1103/PhysRevLett.120.264801

[13] Z. Wang *et al.*, "Nonlinear energy chirp compensation with corrugated structures", *Nucl. Sci. Tech.*, vol. 29, no. 175, p. 1–7, 2018. doi:10.1007/s41365-018-0512-z

[14] S. Bettoni *et al.*, "Experimental demonstration of two-color x-ray free-electron-laser pulses via wakefield excitation", *Phys. Rev. Accel. Beams*, vol. 24, p. 082801, 2021. doi:10.1103/PhysRevAccelBeams.24.082801

[15] J. Duris *et al.*, "Controllable x-ray pulse trains from enhanced self-amplified spontaneous emission", *Phys. Rev. Lett.*, vol. 126, p. 104802, 2021. doi:/10.1103/PhysRevLett.126.104802

[16] Y. Gong *et al.*, "Beam performance of the SHINE dechirper", *Nucl. Sci. Tech.*, vol. 32, no. 29, p. 1–10, 2021. doi:10.1007/s41365-021-00860-8

[17] P. Dijkstal *et al.*, "Self-synchronized and cost-effective time-resolved measurements at x-ray free-electron lasers with femtosecond resolution", *Phys. Rev. Res.*, vol. 4, p. 013017, 2022. doi:10.1103/PhysRevResearch.4.013017

[18] P. Dijkstal *et al.*, "Longitudinal phase space diagnostics with a nonmovable corrugated passive wakefield streaker", *Phys. Rev. Accel. Beams*, vol. 27, p. 050702, 2024. doi:10.1103/PhysRevAccelBeams.27.050702

[19] X. Wang *et al.*, "Physical Design for Shenzhen Superconducting Soft X-ray Free-Electron Laser (S^3FEL)", in *Proc. IPAC'23*, Venice, Italy, May 2023, TUPL043. doi:10.18429/JACoW-IPAC2023-TUPL043

[20] I. Zagorodnov, K. Bane, and G. Stupakov "Calculation of wakefields in 2D rectangular structures", *Phys. Rev. ST Accel. Beams*, vol. 18, p. 104401, 2015. doi:10.1103/PhysRevSTAB.18.104401

[21] CST Studio, CST. https://www.3ds.com/products/simulia/cst-studio-suite

[22] J. Sun *et al.*, "An experimental application of machine learning algorithms to optimize the FEL lasing via beam trajectory tuning at Dalian Coherent Light Source", *Nucl. Instrum. Methods Phys. Res. A*, vol. 1063, p. 169320, 2024. doi:10.1016/j.nima.2024.169320

[23] F. Fu *et al.*, "Demonstration of nonlinear-energy-spread compensation in relativistic electron bunches with corrugated structures", *Phys. Rev. Lett.*, vol. 114, p. 114801, 2015. doi:10.1103/PhysRevLett.114.114801